COLD SPRING HARBOR
Molecular Case Studies

RAPID CANCER COMMUNICATION

Serial liquid biopsies for detection of treatment failure and profiling of resistance mechanisms in *KLC1–ALK*-rearranged lung cancer

Steffen Dietz,[1,2,11] Petros Christopoulos,[2,3,4,11] Lisa Gu,[1,2] Anna-Lena Volckmar,[5] Volker Endris,[5] Zhao Yuan,[6] Simon J. Ogrodnik,[1,2] Tomasz Zemojtel,[7] Claus-Peter Heussel,[2,8] Marc A. Schneider,[2,4] Michael Meister,[2,4] Thomas Muley,[2,4] Martin Reck,[9] Matthias Schlesner,[2,6] Michael Thomas,[2,3] Albrecht Stenzinger,[2,5,10,11] and Holger Sültmann[1,2,11]

[1]Division of Cancer Genome Research, German Cancer Research Center (DKFZ), German Cancer Consortium (DKTK), and National Center for Tumor Diseases (NCT), 69120 Heidelberg, Germany; [2]German Center for Lung Research (DZL), TLRC Heidelberg, 69120 Heidelberg, Germany; [3]Department of Thoracic Oncology, [4]Translational Research Unit, Thoraxklinik at University Hospital Heidelberg, 69120 Heidelberg, Germany; [5]Institute of Pathology, Heidelberg University, 69120 Heidelberg, Germany; [6]Bioinformatics and Omics Data Analytics, German Cancer Research Center (DKFZ), 69120 Heidelberg, Germany; [7]Berlin Institute of Health (BIH) Genomics Core Facility, Charité, University Medical Center, 10017 Berlin, Germany; [8]Diagnostic and Interventional Radiology with Nuclear Medicine, Thoraxklinik at University Hospital Heidelberg, 69120 Heidelberg, Germany; [9]Lung Clinic Grosshansdorf, Airway Research Center North, German Center for Lung Research (DZL), 22927 Großhansdorf, Germany; [10]German Cancer Consortium (DKTK), 69120 Heidelberg, Germany

Abstract Genetic rearrangements involving the anaplastic lymphoma kinase (*ALK*) gene confer sensitivity to ALK tyrosine kinase inhibitors (TKIs) and superior outcome in non-small-cell lung cancer (NSCLC). However, clinical courses vary widely, and recent studies suggest that molecular profiling of ALK$^+$ NSCLC can provide additional predictors of therapy response that could assist further individualization of patient management. As repeated tissue biopsies often pose technical difficulties and significant procedural risk, analysis of tumor constituents circulating in the blood, including ctDNA and various proteins, is increasingly recognized as an alternative method of tumor sampling ("liquid biopsy"). Here, we report the case of a *KLC1–ALK*-rearranged NSCLC patient responding to crizotinib treatment and demonstrate how analysis of plasma and serum biomarkers can be used to identify the *ALK* fusion partner and monitor therapy over time. Results of ctDNA sequencing and copy-number alteration profiling as well as serum protein concentrations at various time points during therapy reflected the current remission status and could predict the subsequent clinical course. At the time of disease progression, we identified four distinct secondary mutations in the *ALK* gene in ctDNA potentially causing treatment failure, accompanied by rising levels of CEA and CYFRA 21–1. Moreover, several copy-number variations were detected at the end of the treatment, including an amplification of a region on Chromosome 12 encompassing the TP53 regulator *MDM2*. In summary, our findings illustrate the utility of noninvasive longitudinal molecular profiling for assessing remission status, exploring mechanisms of treatment failure, predicting subsequent clinical course, and dissecting dynamics of drug-resistant clones in ALK$^+$ lung cancer.

Correspondence:
h.sueltmann@dkfz.de

Ontology term: lung adenocarcinoma

Published by Cold Spring Harbor Laboratory Press

doi:10.1101/mcs.a004630

[11]These authors contributed equally to this work.

CASE PRESENTATION

A 66-yr-old woman without significant comorbidities was diagnosed with metastatic adenocarcinoma of the right lung including ipsilateral pleural and diffuse bone spread (T2N0M1c). Initial treatment with carboplatin/pemetrexed chemotherapy resulted in a partial remission after two cycles and was followed by pemetrexed maintenance. Meanwhile, an *ALK* rearrangement was detected by fluorescence in situ hybridization (FISH). Subsequent RNA next-generation sequencing (NGS) of the tumor identified transcripts of *KLC1* exon 9 fused with *ALK* exon 20 (K9–A20). Retrospective targeted deep sequencing of circulating tumor DNA (ctDNA) from several longitudinal blood plasma samples collected at different time points confirmed the translocation and identified the DNA breakpoints in *KLC1* intron 9 and *ALK* intron 19 (Fig. 1A). The first plasma sample, collected at the time of partial remission after two cycles of carboplatin/pemetrexed chemotherapy, showed a variant allele frequency (VAF) of 0.09% for the *ALK* fusion and no single-nucleotide variants (SNVs) in the *ALK* gene (Fig. 1B). Analysis of a simultaneously collected serum sample revealed a low abundance of CEA (39.52 ng/µL) and CYFRA 21–1 (0.53 ng/µL; Fig. 1C). Two months after initiation of pemetrexed maintenance, the progression of the primary tumor and pleural effusion was noted by chest CT (Fig. 1D, I1), and new cerebral metastases were detected by brain MRI (Fig. 1D, I2). At this timepoint, the retrospectively determined *KLC1–ALK* fusion VAF rose to 6.25% and the tumor protein markers CEA, CYFRA 21–1 were also increased. Second-line treatment with crizotinib (250 bid) was initiated, and the patient initially responded with tumor shrinkage of ~40%, as determined by radiological imaging (Fig. 1D, I3). During the next disease progression with multiple new brain lesions 50 d later (Fig. 1D, I4), the fusion VAF in retrospective analysis was 4.4% (i.e., lower than at the time of the previous systemic progression). However, four distinct secondary mutations in the kinase domain of the *ALK* gene were identified in ctDNA: *ALK* p.F1174C (c.35221T>G) with 0.08% VAF, *ALK* p.F1174L (c.3522C>G with 0.88% VAF and c.3522C>A with 0.24% VAF), and *ALK* p.G1269A (c.3806G>C) with 0.18% VAF (Fig. 1B). After whole-brain radiotherapy with 30 Gy (10 fractions of 3 Gy), clinical and radiological follow-up during the following three months indicated stable disease, wherefore crizotinib treatment was continued. However, a plasma sample taken only 3 wk after the last radiation dose retrospectively revealed rising VAFs of the fusion *KLC1–ALK* (8.01%) and all four secondary *ALK* variants, the most abundant of which was *ALK* p.F1174 (c.3522C>G with 3.26% VAF; Fig. 1B). At the same time, CEA and CYFRA 21–1 concentrations were also elevated (Fig. 1C). In accordance with the rising VAFs and protein levels, and despite the apparently stable radiologic findings, multilocular disease progression occurred just 1 mo later, with multiple new lung and bone metastases as confirmed by PET-CT. Retrospective molecular reassessment with liquid biopsy at that time point showed steadily high VAFs, whereas concentrations of protein markers rose further (CEA: >155 ng/µL, CYFRA 21–2: >200 ng/µL; Fig. 1B,C). Based on the radiologic progression, crizotinib treatment was discontinued and a switch to ceritinib was planned, but the patient died before the therapy could be started. We also performed retrospective shallow whole-genome sequencing (sWGS) of ctDNA from a plasma sample after two cycles of carboplatin/pemetrexed and from the last sample upon progression under crizotinib. Although sWGS of ctDNA during the first months after diagnosis revealed no copy-number variations (CNVs) with a trimmed median absolute deviation from copy-number neutrality (t-MAD) of 0.0098, noticeable alterations were detected at the end of the treatment (t-MAD = 0.0414), including an amplification of the region encompassing the TP53 regulator *MDM2* on Chromosome 12 (Fig. 1C,E).

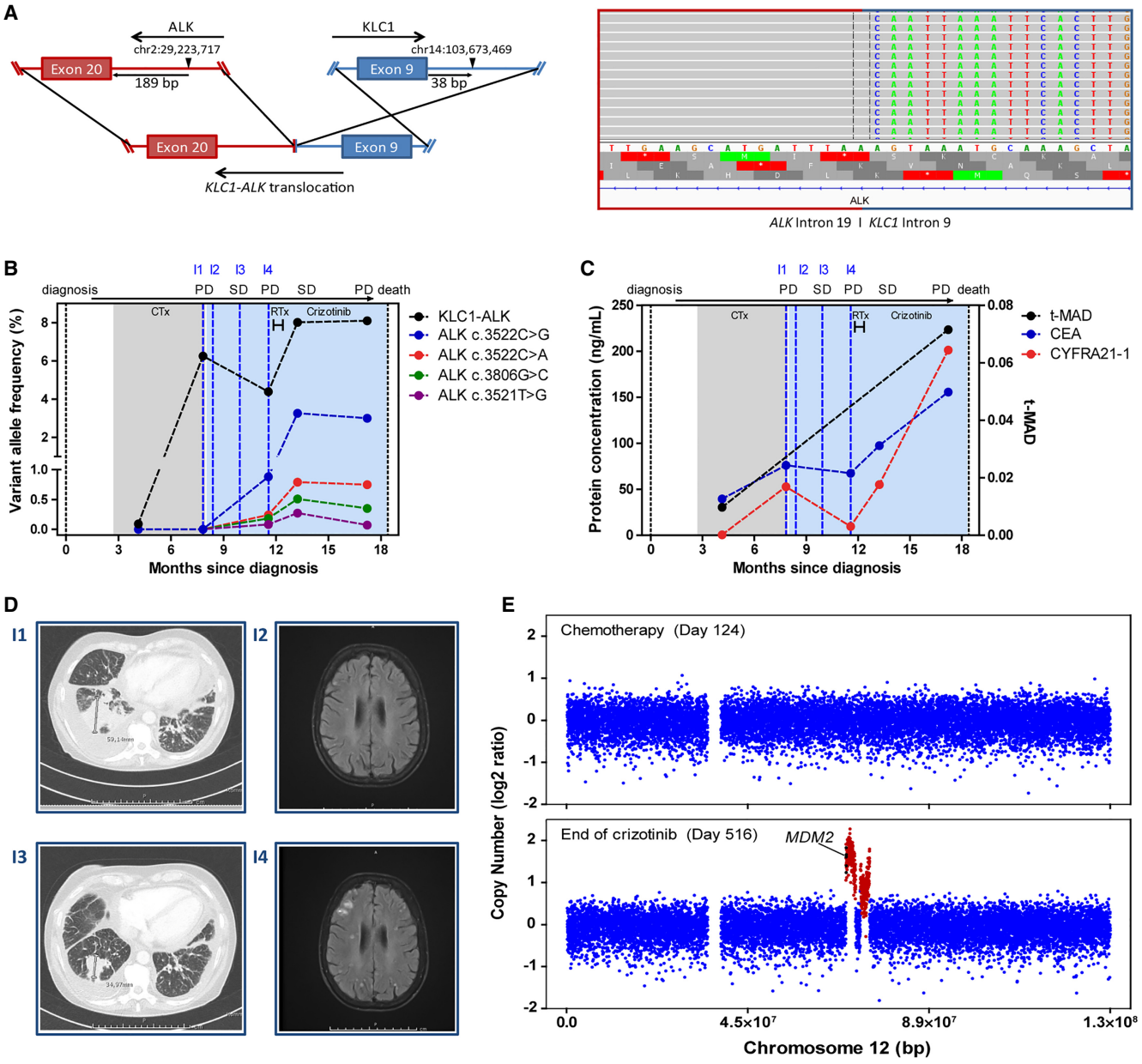

Figure 1. (*A*) Schematic of the predicted genomic translocation of *KLC1–ALK* and aligned ctDNA reads in IGV spanning the rearrangement of *KLC1* intron 8 and *ALK* intron 19. (*B*) Kinetics of mutated allele frequencies detected in ctDNA during treatment. Corresponding images (I1–I4) are shown in *E*. Phases of stable disease and progressive disease are indicated on *top*. (*C*) Kinetics of serum protein concentrations during treatment. Corresponding images (I1–I4) are shown in *D*. Phases of stable disease and progressive disease are indicated on *top*. (*D*) Corresponding chest CT of the primary tumor (on the *left*; I1, I3) and brain MRI images of cerebral metastases (on the *right*; I2, I4) taken during the therapy course. (*E*) Copy-number profiles of Chromosome 12 from sWGS of ctDNA. The *upper* panel shows the CNV profile before crizotinib treatment initiation; the *bottom* panel shows the CNV profile at the end of treatment. (SD) Stable disease, (PD) progressive disease, (CTx) chemotherapy, (RTx) whole-brain radiotherapy.

TECHNICAL ANALYSIS AND METHODS

The histological diagnosis of lung adenocarcinoma was performed by experienced pulmonary pathologists on a formalin-fixed and paraffin-embedded (FFPE) biopsy of the primary tumor. The presence of the *ALK* rearrangement was determined by fluorescent in situ hybridization (FISH) using ALK break-apart probes (ZytoLight SPEC ALK probe, ZytoVision). A fusion transcript with exon 9 of *KLC1* fused to *ALK* exon 20 (K9–A20) was confirmed by RNA NGS using the AmpliSeq RNA Lung Cancer Fusion Panel (Thermo Fisher Scientific) as described previously (Pfarr et al. 2016; Volckmar et al. 2019).

For ctDNA analysis, plasma was isolated from blood samples, centrifuged within 30 min of collection, and processed with the AVENIO ctDNA Analysis Kit according to the manufacturer's instructions (Roche Diagnostics). Briefly, cell-free DNA was isolated from 2 mL of plasma using the AVENIO cfDNA Isolation Kit (Roche) and quantified with the Qubit dsDNA High Sensitivity Kit (Thermo Fisher). Targeted sequencing libraries were prepared from 39.9 ng DNA in median (range 24.5–50 ng) using the AVENIO ctDNA Library Preparation Kit with the AVENIO Targeted and Surveillance Panel (both from Roche) for hybridization-based enrichment of a 17-gene (81-kb) and a 197-gene (198-kb) panel, respectively. Among their target regions, both panels are designed to capture the exons 19 to 28 as well as intron 19 of the *ALK* gene. CtDNA libraries from all plasma samples were initially enriched and sequenced with the AVENIO Targeted panel. To validate variants detected with the Targeted panel and to potentially identify further mutations in an extended genomic target region, all plasma samples were repeatedly enriched and sequenced with the AVENIO Surveillance panel. All protocols were conducted according to the manufacturer's recommendations. Enriched libraries were sequenced on an Illumina NextSeq550 using the High Output Kit V2 (300 cycles) according to the manufacturer's protocol (Illumina) with a median unique target sequence coverage of 7760× (range 4177×–10,869×). Automated raw data processing and data analysis was performed with the AVENIO ctDNA analysis software (Roche). Manual QC of called variants and visualization of aligned reads spanning the DNA breakpoints in *KLC1* intron 9 and *ALK* intron 19 was done using the Integrative Genomics Viewer (IGV) (Robinson et al. 2017).

For low-coverage sWGS, sequencing libraries were prepared from 2.5 ng cell-free DNA using the KAPA Hyper Prep Kit with KAPA Dual-Indexed Adapters for Illumina platforms (both Roche). Following sequencing adapter ligation for 15 h at 16°C to achieve high ligation efficiency, libraries were amplified in 11 PCR cycles and purified according to the manufacturer's protocol. Samples were sequenced in a multiplex of 48 sWGS libraries per lane on an Illumina HiSeq4000 with 100-bp paired-end reads (Illumina). Raw sequencing reads were processed and aligned using the automated pipeline OTP (Reisinger et al. 2017). Genome-wide copy number profiles were estimated from low-coverage sWGS data of ctDNA using ichorCNA (Adalsteinsson et al. 2017), and t-MAD scores were calculated to quantify CNVs (Mouliere et al. 2018).

For protein analysis, serum was isolated from blood samples and centrifuged 30 min after collection to ensure complete coagulation. Serum CEA and CYFRA 21–1 levels were determined from 10 µL of serum by multiplexed flow cytometry using the MILLIPLEX MAP Human Circulating Cancer Biomarker Magnetic Bead Panel (Merck) with the Luminex Bio-Plex 200 immunoassay platform (Bio-Rad). All protocols were conducted according to the manufacturer's recommendations.

Plasma and serum biosamples have been provided by Lungbiobank Heidelberg/BMBH in accordance with the regulations of the BMBH and the approval of the ethics committee of the University of Heidelberg. Analysis of clinical data and tissue and blood samples of the patient in this study was performed after informed consent and approval by the ethics committee of Heidelberg University (S-270/2001 and S-296/2016).

VARIANT INTERPRETATION

The median survival of *ALK*-rearranged non-small-cell lung cancer (ALK$^+$ NSCLC) patients treated with tyrosine kinase inhibitors (TKIs) currently exceeds 5 yr, but clinical courses vary widely (Duruisseaux et al. 2017). Recent studies have demonstrated the association of this clinical heterogeneity with specific molecular tumor characteristics, such as the exact type of *ALK* fusion variant, including non-*EML4* fusions, as well as the presence of *TP53* and other mutations (Christopoulos et al. 2018a,b; Kang et al. 2018; Kron et al. 2018; Christopoulos et al. 2019a,c). Thus, broader molecular profiling of ALK$^+$ NSCLC, using, for example, RNA-/DNA-NGS appears to provide information about several clinically relevant parameters that could be used to optimize therapies and personalized patient treatment beyond the readout obtainable from immunohistochemistry and FISH (Volckmar et al. 2019).

In the lung adenocarcinoma case presented here, a translocation of the *ALK* gene locus was initially detected by FISH analysis. Subsequent RNA sequencing identified fusion transcripts with exon 9 of *KLC1* fused to *ALK* exon 20 (K9–A20), which has been detected only at the RNA level in the past, without any information about TKI sensitivity (Togashi et al. 2012). To the best of our knowledge, our study is the first report of the exact intronic double-strand breakpoints and the resulting interchromosomal rearrangement for a *KLC1–ALK* fusion, which we could identify using hybridization-based deep ctDNA sequencing (Table 1; Fig. 1B). Our results show that the *KLC1–ALK* fusion of our patient encompasses the DNA sequence encoding the 5′-end part of *KLC1*, including the promoter domain, together with the sequence coding for the intracellular part of the ALK protein, including the entire tyrosine kinase domain, suggesting sensitivity to treatment with ALK inhibitors. Indeed, the patient showed a good response to crizotinib with partial tumor remission and is—to the best of our knowledge—the first *KLC1–ALK* NSCLC case successfully treated with ALK TKI in the literature.

At the time of failure for any treatment, be it chemotherapy, crizotinib, or after cerebral radiotherapy (Fig. 1D, I1), disease progression was detectable in liquid biopsies as increasing VAF of the *KLC1–ALK* fusion and rising protein tumor markers. Moreover, at the time of cerebral disease progression with multiple new brain lesions under crizotinib (Fig. 1E,I3), ctDNA assessment identified four distinct mutations in the *ALK* kinase domain, which potentially cause the progression (Table 1; Fig. 1B). Three out of the four (*ALK* c.3522C>G, *ALK* c.3522C>G/A, and c.3521T>G) encode the p.F1174C/L variants, which are associated

Table 1. Genomic findings

Gene	Chr	HGVS DNA ref	HGVS Protein ref	Variant type	Predicted effect	Allele frequency	Target coverage	Mutation read count
KLC1–ALK	2	t(2;14)(p23.1;32.33) (hg19 Chr 2:29,223,717:Chr 14:103,673,469)	n/a	*KLC1–ALK* fusion	Oncogenic, sensitivity to *ALK inhibitor*	8.09%	5860×	474
ALK	2	c.3521T>G	p.F1174C	Substitution	Crizotinib resistance	0.27%	10,316×	28
ALK	2	c.3522C>A	p.F1174L	Substitution	Crizotinib resistance	0.79%	10,192×	81
ALK	2	c.3522C>G	p.P1174L	Substitution	Crizotinib resistance	3.26%	10,192×	332
ALK	2	c.3806G>C	p.G1269A	Substitution	Crizotinib resistance	0.51%	16,190×	83

with resistance to ceritinib and crizotinib (Gainor et al. 2016; Lin et al. 2017). The fourth mutation (*ALK* c.3806G>C) encodes the p.G1269A variant, which is associated with resistance to crizotinib (Gainor et al. 2016). Interestingly, the four secondary mutations show similar courses over time, suggesting a parallel evolution of multiple resistant clones with distinct molecular resistance mechanisms. Although Gainor et al. detected all these resistance mutations in tissue specimens obtained from progressing *EML4–ALK*-rearranged tumors, our report is the first to describe these mutations occurring simultaneously in ctDNA of a *KLC1–ALK* patient progressing under crizotinib. In line with this finding, recent proof-of-concept studies also demonstrated the feasibility of identifying and tracking resistance mutations to ALK inhibitors with serial liquid biopsies (Dagogo-Jack et al. 2018; De Carlo et al. 2018; McCoach et al. 2018), illustrating the potential utility of plasma ctDNA genotyping in the clinical patient management in ALK$^+$ NSCLC (Rolfo et al. 2018). Besides ALK$^+$ NSCLC, several studies demonstrated the potential of ctDNA typing for cancer detection, molecular profiling, therapy monitoring, and identification of treatment resistance in various tumor entities (Murtaza et al. 2013; Abbosh et al. 2017; Wan et al. 2017; Cohen et al. 2018). Finally, although imaging suggested stable disease after radiotherapy with remission of the cerebral lesions, rising ctDNA levels of the *KLC1–ALK* fusion and of all four secondary *ALK* point mutations suggested poor disease control. Importantly, this was accompanied by rising concentrations of both protein tumor markers CEA and CYFRA 21–1 in synchronous serum samples (Fig. 1C), and confirmed by the subsequent clinical course, which showed multifocal radiologic progression a few weeks later in conjunction with further increases in all ctDNA and protein markers.

Panel sequencing utilizes enrichment of specific loci and enables deep sequencing to detect recurrent hotspot or resistance mutations; however, it is limited to mutations within the target regions. In contrast, whole-genome or -exome sequencing of plasma DNA facilitates comprehensive molecular profiling, including de novo mutations and CNVs, but is only feasible for increased ctDNA fractions as the analytical sensitivity is limited by the relatively low coverage. Increasing the tumor-derived fraction of cell-free DNA could help to overcome this limitation and to improve the detection of somatic aberrations at lower sequencing depths (Mouliere et al. 2018). Here, we demonstrate a complementary use of targeted deep sequencing and low-coverage sWGS. In addition to mutation typing, we performed sWGS of cell-free DNA to assess CNV profiles at the genome-scale. Prior to crizotinib initiation, no CNVs were detected in the plasma sample of our patient. In contrast, remarkable alterations with fourfold t-MAD increase were detected at the end of treatment, including an amplification of a region on Chromosome 12 encompassing the TP53 regulator gene *MDM2* (Fig. 1C, E). *MDM2* amplifications have been directly associated with worse prognosis and TKI resistance in *RET*-rearranged lung cancers (Dworakowska et al. 2004; Somwar et al. 2016), whereas impairment of TP53 function, as would be expected with MDM2 overexpression, is an important determinant of poor survival in ALK$^+$ NSCLC, either at baseline or if acquired during the course of the disease (Kron et al. 2018; Christopoulos et al. 2019b,c). Thus, although the presence of the amplification in the baseline cannot be excluded because of the overall low ctDNA fraction in this sample, the findings suggest that CNVs, including the *MDM2* amplification, might contribute to the progression of ALK$^+$ NSCLC patients beyond secondary mutations in the ALK kinase domain.

SUMMARY

We report the first case of *KLC1–ALK*-rearranged lung adenocarcinoma responding to treatment with crizotinib and demonstrate the utility of multiple plasma and serum biomarkers for identification of *ALK* fusion partners and longitudinal disease monitoring in ALK$^+$ NSCLC. At

the time of treatment, failure under chemotherapy, crizotinib and cerebral radiotherapy, rising allelic frequencies of the *ALK* fusion, distinct *ALK* resistance mutations (in case of TKI), emerging CNV, and increasing concentrations of protein markers reflected the poor disease control and predicted the subsequent clinical deterioration, in part earlier and more reliably than radiologic findings. Our findings illustrate the potential clinical utility of noninvasive longitudinal molecular profiling for assessing remission status, exploring mechanisms of treatment failure, predicting subsequent clinical course, and dissecting dynamics of drug-resistant clones in ALK^+ lung cancer.

Competing Interest Statement

S.D. reports speaker's honoraria from Roche; P.C. reports research funding from Novartis, Roche, AstraZeneca, and Takeda, as well as advisory board and/or lecture fees from Boehringer, Pfizer, and Chugai; A.-L.V. reports speaker's honoraria from Astra Zeneca; V.E. reports advisory board and lecture fees from AstraZeneca and Thermo Fisher; M.T. reports advisory board honoraria from Novartis, Lilly, BMS, MSD, Roche, Celgene, Takeda, AbbVie, and Boehringer, speaker's honoraria from Lilly, MSD, and Takeda, research funding from AstraZeneca, BMS, Celgene, Novartis, and Roche, and travel grants from BMS, MSD, Novartis, and Boehringer; A.S. reports advisory board honoraria from BMS, Bayer, AstraZeneca, Thermo Fisher, Novartis, and Seattle Genomics, speaker's honoraria from BMS, Bayer, Illumina, AstraZeneca, Novartis, Thermo Fisher, MSD, and Roche, as well as research funding from Chugai, Bayer, and BMS; and H.S. reports advisory board and speaker's honoraria from Roche.

Referees

Alexander Wyatt
Anonymous

Received July 26, 2019; accepted in revised form September 4, 2019.

ADDITIONAL INFORMATION

Data Deposition and Access

The variants of this case have been submitted to COSMIC (https://cancer.sanger.ac.uk/cosmic) and are available under the accession number COSP46927.

Ethics Statement

Analysis of clinical data and tissue and blood samples of the patient in this study was performed after informed consent and approval by the ethics committee of Heidelberg University (S-270/2001 and S-296/2016).

Acknowledgments

The authors thank Ingrid Heinzmann-Groth and Saskia Östringer of Translational Research Unit (STF) of Thoraxklinik Heidelberg for assistance with the collection of patient samples, the Berlin Institute of Health Core Unit Genomics at the Charité and the Genomics and Proteomics Core Facility at the German Cancer Research Center (DKFZ) for sequencing analyses, and the Omics IT and Data Management Core Facility at the German Cancer Research Center (DKFZ) for data management and processing. The authors also thank Gregor Obernosterer (Roche Diagnostics) for logistic support.

Author Contributions

S.D., P.C., L.G., M.T., A.S., and H.S. designed the study. P.C., M.R., and M.T. were responsible for patient treatment. S.D., P.C., L.G., A.-L.V., C.-P.H., S.J.O., T.Z., M.A.S., M.M., T.M., M.R., M.T., A.S., and H.S. processed the samples. S.D., P.C., L.G., A.-L.V., V.E., Z.Y., T.Z., M.S., M.T., A.S., and H.S. analyzed the data. All authors wrote and revised the manuscript.

Funding

This work was supported by the German Center for Lung Research (DZL), by the German Cancer Consortium (DKTK), by the Heidelberg Center for Personalized Oncology at the German Cancer Research Center (DKFZ-HIPO), and by Roche Molecular Solutions.

REFERENCES

Abbosh C, Birkbak NJ, Wilson GA, Jamal-Hanjani M, Constantin T, Salari R, Le Quesne J, Moore DA, Veeriah S, Rosenthal R, et al. 2017. Phylogenetic ctDNA analysis depicts early-stage lung cancer evolution. *Nature* **545:** 446–451. doi:10.1038/nature22364

Adalsteinsson VA, Ha G, Freeman SS, Choudhury AD, Stover DG, Parsons HA, Gydush G, Reed SC, Rotem D, Rhoades J, et al. 2017. Scalable whole-exome sequencing of cell-free DNA reveals high concordance with metastatic tumors. *Nat Commun* **8:** 1324. doi:10.1038/s41467-017-00965-y

Christopoulos P, Endris V, Bozorgmehr F, Elsayed M, Kirchner M, Ristau J, Buchhalter I, Penzel R, Herth FJ, Heussel CP, et al. 2018a. *EML4-ALK* fusion variant V3 is a high-risk feature conferring accelerated metastatic spread, early treatment failure and worse overall survival in ALK$^+$ non–small cell lung cancer. *Int J Cancer* **142:** 2589–2598. doi:10.1002/ijc.31275

Christopoulos P, Kirchner M, Endris V, Stenzinger A, Thomas M. 2018b. *EML4-ALK* V3, treatment resistance, and survival: refining the diagnosis of ALK$^+$ NSCLC. *J Thoracic Dis* **10:** S1989–S1991. doi:10.21037/jtd.2018.05.61

Christopoulos P, Budczies J, Kirchner M, Dietz S, Sültmann H, Thomas M, Stenzinger A. 2019a. Defining molecular risk in ALK$^+$ NSCLC. *Oncotarget* **10:** 3093–3103. doi:10.18632/oncotarget.26886

Christopoulos P, Dietz S, Kirchner M, Volckmar AL, Endris V, Neumann O, Ogrodnik S, Heussel CP, Herth FJ, Eichhorn M, et al. 2019b. Detection of *TP53* mutations in tissue or liquid rebiopsies at progression identifies ALK$^+$ lung cancer patients with poor survival. *Cancers (Basel)* **11:** E124. doi:10.3390/cancers11010124

Christopoulos P, Kirchner M, Bozorgmehr F, Endris V, Elsayed M, Budczies J, Ristau J, Penzel R, Herth FJ, Heussel CP, et al. 2019c. Identification of a highly lethal V3$^+$TP53$^+$ subset in ALK$^+$ lung adenocarcinoma. *Int J Cancer* **144:** 190–199. doi:10.1002/ijc.31893

Cohen JD, Li L, Wang Y, Thoburn C, Afsari B, Danilova L, Douville C, Javed AA, Wong F, Mattox A, et al. 2018. Detection and localization of surgically resectable cancers with a multi-analyte blood test. *Science (80-)* **359:** 926–930. doi:10.1126/science.aar3247

Dagogo-Jack I, Brannon AR, Ferris LA, Campbell CD, Lin JJ, Schultz KR, Ackil J, Stevens S, Dardaei L, Yoda S, et al. 2018. Tracking the evolution of resistance to ALK tyrosine kinase inhibitors through longitudinal analysis of circulating tumor DNA. *JCO Precis Oncol* **2018**. doi:10.1200/PO.17.00160

De Carlo E, Schiappacassi M, Urbani M, Doliana R, Baldassarre G, Da Ros V, Santarossa S, Chimienti E, Berto E, Fratino L, et al. 2018. Therapeutic decision based on molecular detection of resistance mechanism in an ALK-rearranged lung cancer patient: a case report. *Onco Targets Ther* **11:** 8945–8950. doi:10.2147/OTT.S184745

Duruisseaux M, Besse B, Cadranel J, Pérol M, Mennecier B, Bigay-Game L, Descourt R, Dansin E, Audigier-Valette C, Moreau L, et al. 2017. Overall survival with crizotinib and next-generation ALK inhibitors in *ALK*-positive non-small-cell lung cancer (IFCT-1302 CLINALK): a French nationwide cohort retrospective study. *Oncotarget* **8:** 21903–21917. doi:10.18632/oncotarget.15746

Dworakowska D, Jassem E, Jassem J, Peters B, Dziadziuszko R, Żylicz M, Jakóbkiewicz-Banecka J, Kobierska-Gulida G, Szymanowska A, Skokowski J, et al. 2004. *MDM2* gene amplification: a new independent factor of adverse prognosis in non–small cell lung cancer (NSCLC). *Lung Cancer* **43:** 285–295. doi:10.1016/j.lungcan.2003.09.010

Gainor JF, Dardaei L, Yoda S, Friboulet L, Leshchiner I, Katayama R, Dagogo-Jack I, Gadgeel S, Schultz K, Singh M, et al. 2016. Molecular mechanisms of resistance to first- and second-generation ALK inhibitors in *ALK*-rearranged lung cancer. *Cancer Discov* **6:** 1118–1133. doi:10.1158/2159-8290.CD-16-0596

Kang J, Zhang XC, Chen HJ, Zhou Q, Tu HY, Li WF. 2018. Uncommon ALK fusion partners in advanced ALK-positive non-small-cell lung cancer. *J Clin Oncol* **36:** 8561. doi:10.1200/JCO.2018.36.15_suppl.8561

Kron A, Alidousty C, Scheffler M, Merkelbach-Bruse S, Seidel D, Riedel R, Ihle MA, Michels S, Nogova L, Fassunke J, et al. 2018. Impact of *TP53* mutation status on systemic treatment outcome in *ALK*-rearranged non-small-cell lung cancer. *Ann Oncol* **29:** 2068–2075. doi:10.1093/annonc/mdy333

Lin JJ, Riely GJ, Shaw AT. 2017. Targeting ALK: precision medicine takes on drug resistance. *Cancer Discov* **7:** 137–155. doi:10.1158/2159-8290.CD-16-1123

McCoach CE, Blakely CM, Banks KC, Levy B, Chue BM, Raymond VM, Le AT, Lee CE, Diaz J, Waqar SN, et al. 2018. Clinical utility of cell-free DNA for the detection of *ALK* fusions and genomic mechanisms of ALK inhibitor resistance in non-small cell lung cancer. *Clin Cancer Res* **24:** 2758–2770. doi:10.1158/1078-0432.CCR-17-2588

Mouliere F, Chandrananda D, Piskorz AM, Moore EK, Morris J, Ahlborn LB, Mair R, Goranova T, Marass F, Heider K, et al. 2018. Enhanced detection of circulating tumor DNA by fragment size analysis. *Sci Transl Med* **10:** eaat4921. doi:10.1126/scitranslmed.aat4921

Murtaza M, Dawson SJ, Tsui DWY, Gale D, Forshew T, Piskorz AM, Parkinson C, Chin SF, Kingsbury Z, Wong ASC, et al. 2013. Non-invasive analysis of acquired resistance to cancer therapy by sequencing of plasma DNA. *Nature* **497:** 108–112. doi:10.1038/nature12065

Pfarr N, Stenzinger A, Penzel R, Warth A, Dienemann H, Schirmacher P, Weichert W, Endris V. 2016. High-throughput diagnostic profiling of clinically actionable gene fusions in lung cancer. *Genes Chromosomes Cancer* **55:** 30–44. doi:10.1002/gcc.22297

Reisinger E, Genthner L, Kerssemakers J, Kensche P, Borufka S, Jugold A, Kling A, Prinz M, Scholz I, Zipprich G, et al. 2017. OTP: an automatized system for managing and processing NGS data. *J Biotechnol* **261:** 53–62. doi:10.1016/j.jbiotec.2017.08.006

Robinson JT, Thorvaldsdóttir H, Wenger AM, Zehir A, Mesirov JP. 2017. Variant review with the integrative genomics viewer. *Cancer Res* **77:** E31–E34. doi:10.1158/0008-5472.CAN-17-0337

Rolfo C, Mack PC, Scagliotti GV, Baas P, Barlesi F, Bivona TG, Herbst RS, Mok TS, Peled N, Pirker R, et al. 2018. Liquid biopsy for advanced non–small cell lung cancer (NSCLC): a statement paper from the IASLC. *J Thorac Oncol* **13:** 1248–1268. doi:10.1016/j.jtho.2018.05.030

Somwar R, Smith R, Hayashi T, Ishizawa K, Charen AS, Khodos I, Mattar M, He J, Balasubramanian S, Stephens P, et al. 2016. *MDM2* amplification (Amp) to mediate cabozantinib resistance in patients (Pts) with advanced *RET*-rearranged lung cancers. *J Clin Oncol* **34:** 9068. doi:10.1200/JCO.2016.34.15_suppl.9068

Togashi Y, Soda M, Sakata S, Sugawara E, Hatano S, Asaka R, Nakajima T, Mano H, Takeuchi K. 2012. KLC1-ALK: a novel fusion in lung cancer identified using a formalin-fixed paraffin-embedded tissue only. *PLoS One* **7:** e31323. doi:10.1371/journal.pone.0031323

Volckmar AL, Leichsenring J, Kirchner M, Christopoulos P, Neumann O, Budczies J, de Oliveira CMM, Rempel E, Buchhalter I, Brandt R, et al. 2019. Combined targeted DNA and RNA sequencing of advanced NSCLC in routine molecular diagnostics: analysis of the first 3,000 Heidelberg cases. *Int J Cancer* **145:** 649–661. doi:10.1002/ijc.32133

Wan JCM, Massie C, Garcia-Corbacho J, Mouliere F, Brenton JD, Caldas C, Pacey S, Baird R, Rosenfeld N. 2017. Liquid biopsies come of age: towards implementation of circulating tumour DNA. *Nat Rev Cancer* **17:** 223–238. doi:10.1038/nrc.2017.7

Serial liquid biopsies for detection of treatment failure and profiling of resistance mechanisms in *KLC1*–*ALK*-rearranged lung cancer

Steffen Dietz, Petros Christopoulos, Lisa Gu, et al.

Cold Spring Harb Mol Case Stud 2019, **5:** a004630 originally published online November 21, 2019
Access the most recent version at doi:10.1101/mcs.a004630